

Research Article

Development of Photocatalytic Active TiO₂ Surfaces by Thermal Spraying of Nanopowders

Filofteia-Laura Toma,¹ Ghislaine Bertrand,² Didier Klein,² Cathy Meunier,³ and Sylvie Begin⁴

¹Fraunhofer Institute Material and Beam Technology (IWS), Winterbergstrasse 28, 01277 Dresden, Germany

²Laboratoire d'Etudes et de Recherches sur les Matériaux, les Procédés et les Surfaces (LERMPS), Université de Technologie de Belfort-Montbéliard (UTBM), Site de Sévenans, 90010 Belfort Cedex, France

³Institut FEMTO-ST (CNRS UMR 6174), 4 Place Tharradin, BP 71427, 25211 Montbéliard, France

⁴ECPM-IPCMS-GMI (CNRS UMR 7504), 23 Rue du Loess, BP 43, 67034 Strasbourg, France

Correspondence should be addressed to Filofteia-Laura Toma, filofteia-laura.toma@iws.fraunhofer.de

Received 4 September 2007; Accepted 13 December 2007

Recommended by Ping Xiao

Titanium dioxide is a very useful photocatalyst for the decomposition and diminution of environmental water and air pollutants. In such applications, it can be used as slurry or as immobilized coating obtained by different deposition methods. The studies performed in the last years showed that thermal spraying could be employed to elaborate TiO₂ coatings with high performance for the decomposition of organic compounds. This manuscript presents a comparative study on the microstructure and photocatalytic performance of titania coatings obtained by different thermal spray techniques: atmospheric plasma spraying (APS), suspension plasma spraying (SPS), and high-velocity oxygen fuel spray process (HVOF). Different titania powders and suspensions were used to study the influence of the feedstock materials on the coating characteristics. The deposits were mainly characterised by SEM and X-ray diffraction. The photocatalytic performance was evaluated from the removal of nitrogen oxides. The experimental results showed that a drastic reduction of the pollutant concentration was obtained in presence of coatings elaborated by suspension plasma spraying. TiO₂ coatings resulting from the spraying of agglomerated powder presented less efficiency. That was mainly explained by the significant phase transformation from anatase to rutile that occurred in the enthalpic source during the spray processes.

Copyright © 2008 Filofteia-Laura Toma et al. This is an open access article distributed under the Creative Commons Attribution License, which permits unrestricted use, distribution, and reproduction in any medium, provided the original work is properly cited.

1. INTRODUCTION

Titanium dioxide (TiO₂) is an attractive material for numerous technological processes. It finds applications as gas sensors, as pigments in foodstuffs, paints, cosmetics, or pharmacology, as a corrosion resistant coating, in heterogeneous catalysis and photocatalysis, in solar cells for the production of hydrogen and electric energy, in electronic devices, and so on. After the initial work by Fujishima and Honda [1] on the photolysis of water on TiO₂ electrodes, extensive studies on titania photochemical applications have been carried out in the last few decades. As a photocatalyst, titanium dioxide can be used in the degradation of air and water pollutants, in medical sterilization, and even in cancer therapy [2–4]. Among the two TiO₂ crystalline phases, anatase and rutile that can contribute to the photocatalysis, it is generally assumed that the anatase—the metastable phase, which

by thermal treatment irreversibly turns into rutile—allows a higher-photocatalytic degradation of the pollutants. However, some anatase powders containing small quantities of rutile present a better efficiency than those of pure anatase [5, 6]. For the photocatalytic applications, titanium dioxide can be used in powder form (slurry) or immobilized in thin film or coating form obtained by different deposition techniques (sol-gel, dip-coating, and physical or chemical vapour deposition, etc.). TiO₂ powders have an outstanding photocatalytic efficiency compared with their coating counterparts due to their higher specific surface area. However, the separation of powder from the liquid state used in water treatments and recycling processes is troublesome, mainly because of the formation of aggregates. On the other hand, it is considered that the aforementioned difficulties concerning films and coatings can be overcome and their applications can also be expanded by employing various materials as substrates.

Thermal spraying is widely used to prepare titania coatings for mechanical and biomedical applications due to their hardness, wear and corrosion resistance, and biocompatibility [7–12]. The studies performed in the last years showed that the thermal spray technique could be employed to obtain TiO₂ coatings with an effective photocatalytic performance for the decomposition of organic compounds [13–16].

In thermal spraying, the material feedstock (commonly a powder with typical particles size distribution ranging from 10 to 100 μm) is injected in an enthalpic source (thermal plasma or flame obtained by ionization-excitation of inert gases or combustion, resp.). The particles are melted (or partially melted), accelerated by a gas flow, and crushed on the target substrate where rapid solidification and deposit built-up occur. In the last years, a new technique, called liquid thermal spraying, with liquid materials as feedstock precursors was developed [17–24]. The liquid precursors can be (i) organic (ethoxide, butoxide, acetate, etc.) or inorganic (nitrate, chloride, etc.) solutions, and (ii) aqueous or alcoholic suspensions of the material to be sprayed. The suspension allows the feeding of particles with diameters ranging from several nm to 1 μm into the plasma plume. To be used as a precursor in thermal spraying, the slurry (suspension of fine particles in a solvent) has to contain a high-powder load with a low viscosity and a high stability. The deposition depends on different parameters such as the hydrodynamic properties of the liquid which depend on the solid content, droplet diameters, and thermal and kinetics history of the droplets before impinging on the substrate [25].

In this paper, a comparative study on the microstructure and photocatalytic performance of the nanostructured TiO₂ coatings obtained by different thermal spray techniques: atmospheric plasma spraying (APS), suspension plasma spraying (SPS), and high-velocity oxygen fuel (HVOF) spray process is proposed. The coating microstructure was mainly characterized by scanning electron microscopy and X-ray diffraction. The photocatalytic behavior of sprayed coatings was evaluated by a degradation of gaseous nitrogen oxide pollutants (NO, NO_x), major air pollutants that cause serious problems on the environment and human health.

2. EXPERIMENTAL PROCEDURE

2.1. Material feedstock

Three commercial TiO₂ powders were used in this study: a pure anatase nanopowder, with 7 nm crystalline size, namely, TiO₂-ST01 (Ishihara Sangyo, Japan) agglomerated by spray-drying in order to prepare spherical microsized anatase particles (with a size distribution ranging from 10 to 50 μm); a 23 nm anatase nanopowder TiO₂-PC105 (Millennium Inorganic Chemicals, France) and TiO₂-P25 powder (Degussa AG, Germany) generally considered as a reference in the photocatalytic applications, containing 80 vol.% anatase (25 nm) and 20 vol.% rutile (50 nm).

Distilled water and ethylic alcohol were used as solvents in the preparation of suspensions, in which the powder load

was set to 20–25 wt%. No dispersing agent was added in the composition of the suspensions.

2.2. Thermal spraying

Different thermal spray techniques were used to elaborate nanostructured coatings. Moreover, the spray conditions had been adjusted in order to minimize the particle heat input and to maintain the original anatase phase in the elaborated coating.

Atmospheric plasma spraying (APS) was carried out with a Sulzer-Metco PTF4 plasma gun (6 mm nozzle torch). Ar at 40 L·min⁻¹ was used as primary plasma gas; H₂ (3 L·min⁻¹) and He (20 L·min⁻¹) were added as secondary plasma gases. The arc intensity was about 400 A. Stainless steel substrates (60 × 70 × 2 mm³) previously sand-blasted were set to 80 and 100 mm from the exit of the nozzle torch. The powder rate was 14 g·min⁻¹ and carried by Ar at 3 L·min⁻¹.

A special device was designed for the injection of liquid in the plasma [26]. The suspensions were introduced by a peristaltic pump, at a feed rate of about 20–25 mL·min⁻¹, in the system that ensured the atomization of the liquid and radial injection of the resulting drops in the plasma jet (Figure 1). Argon at a flow rate of 3–5 L·min⁻¹ allowed the atomization of the liquid before entering in the plasma.

High-velocity oxygen flame spraying (HVOF spraying) was performed with a Sulzer-Metco CDS 100 gun (with a 3-inche nozzle) using natural methane, as fuel gas. The flame was obtained by the combustion of 100 L·min⁻¹ CH₄ with 400 L·min⁻¹ O₂. N₂ at a flow rate of 50 L·min⁻¹ was also added to the gas mixture to decrease the flame temperature. The powder feed rate was 20 g·min⁻¹ and was carried by N₂ at a flow rate of 9.5 L·min⁻¹. The spray distance was set to 150 mm.

2.3. Characterisation

The coatings morphology was examined using a JEOL JSM-5800 LV scanning electron microscopy. X-ray diffraction (X'Pert MPD Philips diffractometer) with Cu Kα radiation was used to assess the anatase to rutile ratio. Scan step was 0.02° s⁻¹ with a step time of 0.5 second in the 20–90° 2θ range. The volume percentage of anatase was determined according to the relation developed by Berger-Keller et al. [27]. $C_A = 8I_A / (8I_A + 13I_R)$, where I_A and I_R are the X-ray intensities of the anatase (1 0 1) and rutile (1 1 0) peaks, respectively. The crystallite size was evaluated from the X-ray diffraction based on the Scherrer formula.

The photocatalytic performance of TiO₂ was evaluated by the decrease of nitrogen oxides (NO, NO_x) concentration in a purpose-built test chamber described elsewhere [28]. A 15-W daylight lamp with a fraction of 30% UVA and 4% UVB ensured the irradiation of the TiO₂. The NO and NO_x concentrations were measured continuously using an AC-30M NO_x dual chamber analyzer (environmental SA, France) and recorded with a data acquisition system.

The photocatalytic tests were performed over the sprayed coatings and the initial powders. The photocatalytic performances were evaluated as the ratio of the photocatalytic

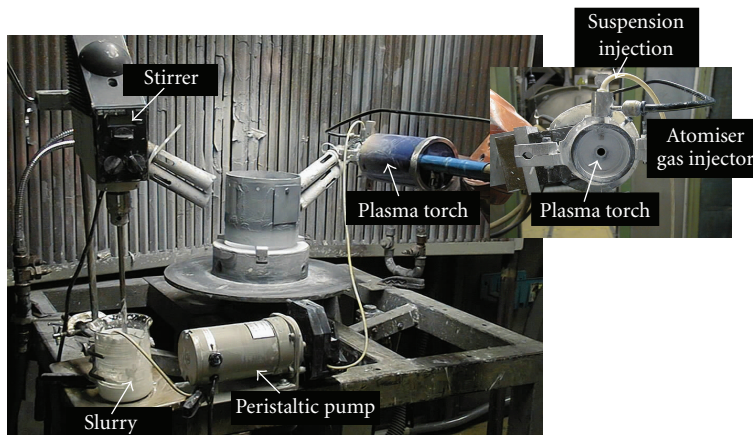


FIGURE 1: Suspension plasma spraying setup.

conversion of nitrogen oxides and determined by the following relations:

$$\text{NO conversion (\%)} = \frac{[\text{NO}]_{\text{initial}} - [\text{NO}]_{\text{UV}}}{[\text{NO}]_{\text{initial}}} \times 100,$$

$$\text{NOx conversion (\%)} = \frac{[\text{NOx}]_{\text{initial}} - [\text{NOx}]_{\text{UV}}}{[\text{NOx}]_{\text{initial}}} \times 100,$$
(1)

where NO conversion (%) and NOx conversion (%) were the photocatalytic removal of NO and NOx concentrations in the presence of the catalyst and UV irradiation; $[\text{NO}]_{\text{initial}}$ and $[\text{NOx}]_{\text{initial}}$ represented the values of the NO and NOx concentrations without UV irradiation; $[\text{NO}]_{\text{UV}}$ and $[\text{NOx}]_{\text{UV}}$ were the values of the NO and NOx concentrations under UV irradiation.

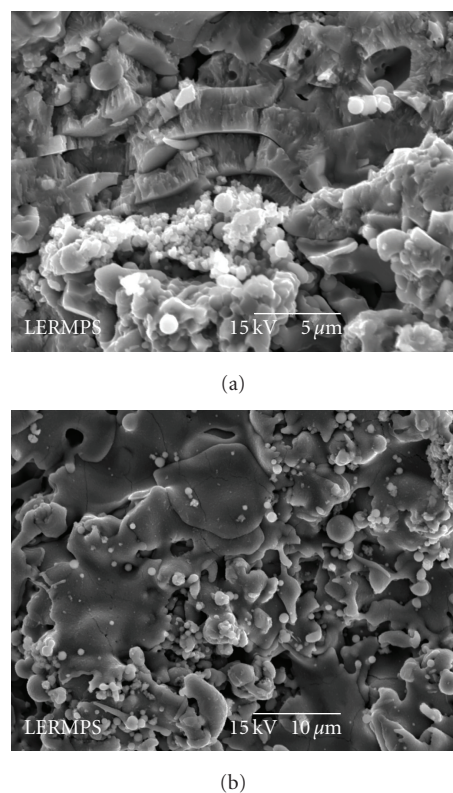
3. RESULTS AND DISCUSSION

3.1. Coating microstructure

3.1.1. Plasma spraying

The morphology of the sprayed coating was mainly dependent on the thermal spray technique. The deposits obtained by the plasma spraying of the agglomerated TiO_2 -ST01 nanopowder were characterized by a bimodal microstructure (Figure 2): on the one hand, a thin lamellar morphology commonly observed with sprayed coatings that contained fully melted particles, and on the other hand, a structure of densely agglomerated grains that contained partially melted particles.

When the agglomerated ST01 nanopowder was dispersed in distilled water (25 wt% powder loading) and injected in the plasma jet as a suspension, the microstructure of the resulting coatings did not present the lamellar structure, which is a characteristic of the thermal sprayed coatings. The TiO_2 -ST01 suspension-sprayed coatings were relatively porous and constituted of partially melted or unmelted fine particles as depicted in Figure 3. The different microstructure

FIGURE 2: SEM-microstructures of nanostructured TiO_2 -ST01 coating prepared by APS technique: (a) fracture; (b) surface.

of the ST01 coatings elaborated by suspension plasma spraying compared with their counterparts obtained from conventional APS was explained by the fact that the thermal transfer between the plasma jet and the material was less important when the suspension was used as feedstock material. In this case, a part of the plasma energy was used to evaporate the solvent of the suspension droplets; the flying time of the resulting particles (free of liquid) was not enough to ensure a complete melting of the particles before impact on substrate.

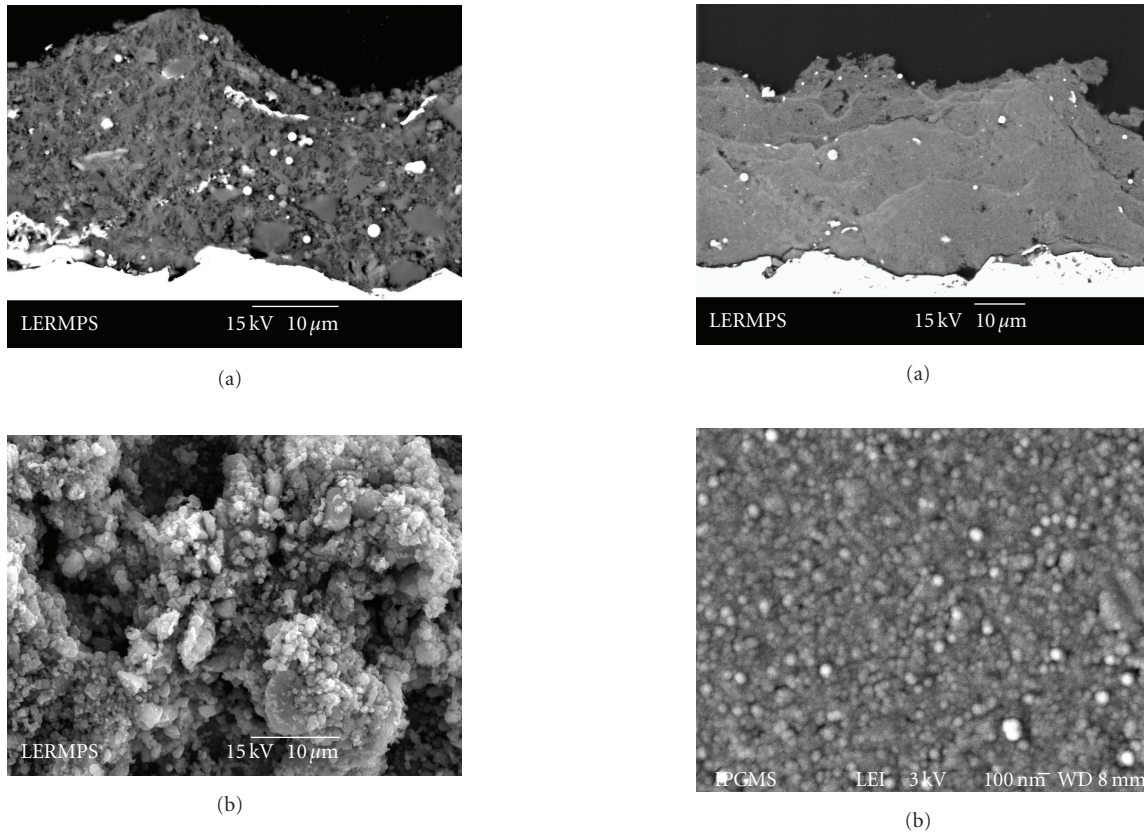


FIGURE 3: SEM-microstructures of TiO_2 -ST01 coating prepared by suspension plasma technique: (a) cross-section; (b) surface.

A nonlamellar microstructure was also observed in the coatings obtained by the plasma spraying of the suspensions (20 wt% powder loading) of nonagglomerated titania powders P25 and PC105. The coatings formed from aqueous suspensions exhibited relatively dense structures (see Figure 4). Moreover, it seemed, at high-microscopic scale, that the coatings were built up by the dense stacking up of fine spherical nanoparticles [29].

Different morphologies were observed in the case of the deposits elaborated from alcoholic suspensions of the two titania nonagglomerated powders. TiO_2 -P25 alcoholic suspension-sprayed coating contained melted and nonmelted particles as shown in Figure 5(a). The presence of the melted zones was explained by the fact that the enthalpy of the evaporation of ethanol was lower ($0.8 \cdot 10^6$ J/kg) than that of water ($2.3 \cdot 10^6$ J/kg). Moreover, it was claimed that the injection of an alcoholic suspension in the plasma plume was assumed to increase the jet temperature as well as the gas speed [25]. In this case, the thermal transfer between the plasma and the particles was more important so the particles were easily heated and then melted. Thus, the molten particles had enough momentum to impinge on the substrate and spread out in splat forms like usually achieved in thermal spray process.

The coatings produced from an alcoholic suspension of PC105 particles were porous; different microstructural fea-

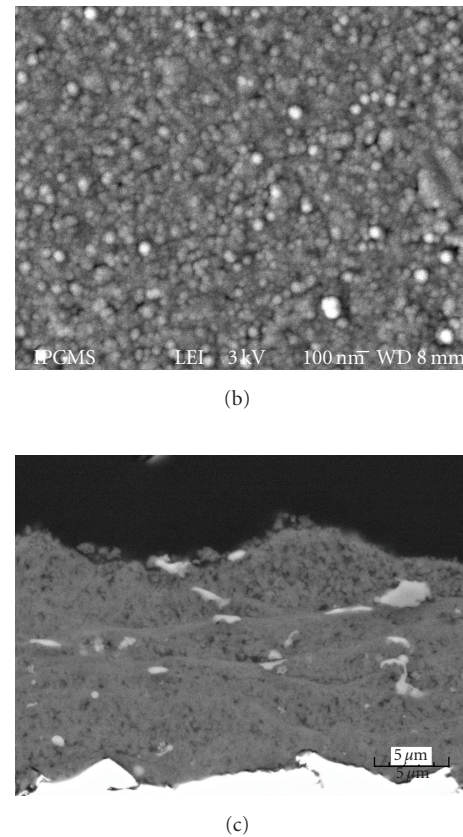
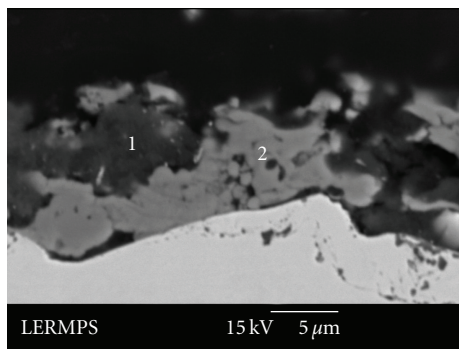
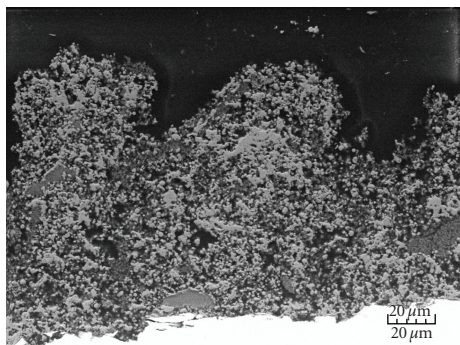


FIGURE 4: SEM-morphology of coatings starting from aqueous suspensions of (a) TiO_2 -P25; (b) TiO_2 -P25 at high-microscopic scale; (c) TiO_2 -PC105 [29].

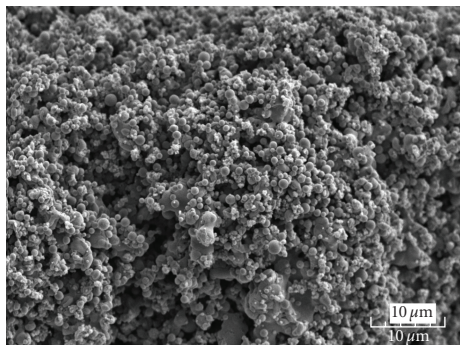
tures were distinguished on the cross-section of the coating: fully melted zones, nonmelted regions, and spherical particles (Figures 5(b), 5(c)). These features were explained by the large distribution of the liquid droplets injected in the plasma as well as the different thermal history of the particles in the enthalpic source before impinging on the substrate. It was interesting to notice the very different microstructures of these coatings compared to that resulting from the P25 alcoholic suspension. This structure was probably due to the different physical properties of the suspensions such as viscosity or surface tension.



(a)



(b)

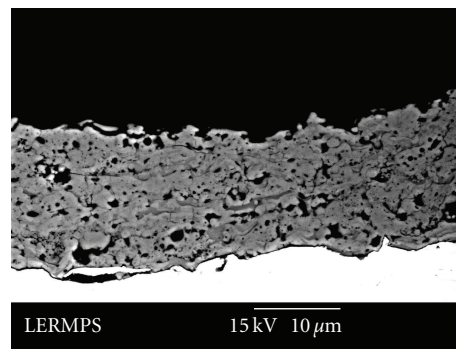


(c)

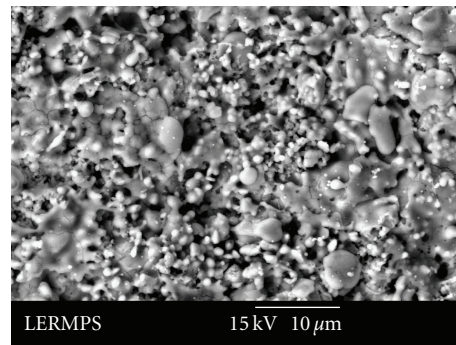
FIGURE 5: SEM-morphology of coatings starting from alcoholic suspensions of (a) TiO_2 -P25, cross-section (1: unmelted regions; 2: melted zones); (b) TiO_2 -PC105, cross-section; (c) TiO_2 -PC105, surface.

3.1.2. HVOF spraying

The TiO_2 deposits elaborated by the HVOF spraying of agglomerated TiO_2 -ST01 nanopowder were porous and characterized by a layered structure (Figure 6). The coatings were mainly built up by the melted nanoparticles impacting on the substrate that flatten to form splats which are consecutively piled on top of the others. Some partially molten particles embedded in the coating structure were also observed. The surface analysis showed the presence of fine particles which conserved the initial features of the agglomerated TiO_2 -ST01 nanopowder.



(a)



(b)

FIGURE 6: SEM-microstructures of TiO_2 -ST01 coating prepared by HVOF technique: (a) cross-section; (b) surface.

3.2. Coating crystalline structure

X-ray diffraction was performed to assess the anatase to rutile ratio. The analysis showed that the passage of the feedstock material (as particles or liquid suspension) in the enthalpic source (plasma or flame) involved the modifications of the chemical state of titanium dioxide compared to that of the initial powders. These structural transformations depended on the thermal spray method used in the elaboration of TiO_2 coatings.

Table 1 resumes the crystalline phases and the crystalline size of the particles determined in different sprayed coatings. The coating elaborated by the plasma spraying of agglomerated ST01 powder contained the rutile structure as a major phase; the anatase content was estimated between 10.9 and 12.2 vol.%. Some traces of TiO_x or Magnéli phases were also identified. The crystallite sizes of the anatase increased from 7 nm to 34 nm. An important phase transformation from anatase to rutile was also observed in the coating obtained by HVOF process. In contrast, when the agglomerated ST01 powder was injected in the plasma in form of aqueous suspension, the content of anatase phase was higher than 96 vol.%; furthermore, the crystalline size of anatase was preserved (7.0–7.3 nm), practically identical to that of the original powder.

The crystalline structure of the coating was relative to the melting degree of the particles during spraying. It is generally accepted that the rutile phase corresponds to the fully melted

TABLE 1: Phases and crystallites size in the thermal sprayed coatings.

Ref. TiO ₂ coating	Anatase (vol.%)	Anatase crystallites average size (nm)	Rutile crystallites average size (nm)	Observations (other phases)
ST01-APS	10.9–12.2	19.2–34.8	67.0–78.6	Traces of Magnéli phases (Ti ₃ O ₅ ; Ti ₆ O ₁₁)
ST01-WSC*	>96.0	7.0–7.3	0–25.1	—
ST01-HVOF	12.6	80.0	90.0	—
P25-WSC	77.6–81.4	27.1–29.2	51.7–60.5	—
P25-ASC**	23.0	46.0	120.0	—
PC105-WSC	91.9–95.1	34.9–38.7	140.9–194.9	—
PC105-ASC	36.2	151.1	99.2	—

*WSC-coating resulted from plasma spraying of aqueous suspension.

** ASC-coating resulted from plasma spraying of alcoholic suspension.

particles, whereas the anatase structure was mostly presented in the partially and nonmelted particles [13].

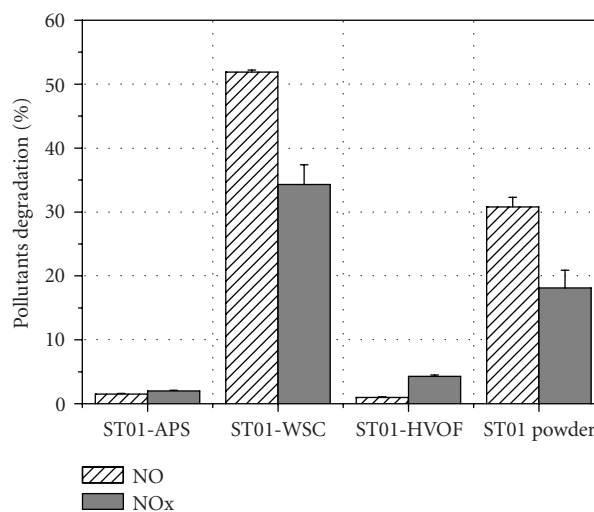
With an aqueous suspension of the agglomerated ST01 nanopowder, the phase transformation was avoided because a part of the plasma energy was used to vaporize the water contained in the liquid droplets. So, the flight time in the plasma jet was not long enough so that the anatase to rutile structural transformation occurred before the particle impact on the substrate.

In the case of suspension spraying of nonagglomerated TiO₂ nanopowders, the XRD analysis showed that the anatase ratio depended on the nature of the solvent (water or alcohol) used in the suspension preparation. The plasma spraying of an aqueous slurry led to coatings where the anatase content and the average crystallite size were almost the same as those identified in the raw powders. On the other hand, the injection of alcoholic suspensions involved the structural transformation from anatase to rutile (about 23 vol.% for P25-coatings and 36 vol.% for PC105 coatings), as well as the increase of the crystallite size of the anatase from 23–25 nm to 150 nm. In this case, the phase transformation was attributed to an easier fragmentation of the alcoholic slurry (due to a lower surface tension of the ethanol), followed by a rapid vaporization of the ethanol. Thus, the flight time of the resulting particles had to be long enough to ensure the partial structural transformation from anatase to rutile.

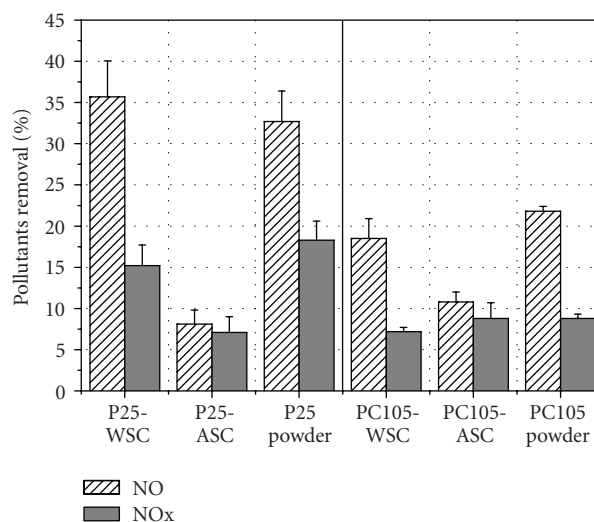
3.3. Photocatalytic performance for the degradation of nitrogen oxides

The photocatalytic properties of the sprayed coatings were evaluated by the diminution of gaseous nitrogen oxides and compared with those obtained in the presence of the corresponding powders. 0.4 g of each powder was uniformly distributed over the entire geometric surface of a Petri dish with 54 cm² surface area.

The photocatalytic activities of TiO₂ coatings are represented in Figure 7. Different behaviors in the photocatalytic performances were noticed depending on the spraying parameters and nature of the material feedstock.



(a)



(b)

FIGURE 7: Photocatalytic degradation of nitrogen oxides in presence of coatings elaborated from (a) agglomerated ST01 nanopowder; (b) nonagglomerated P25 and PC105 nanopowders.

A very low degradation of nitrogen oxide pollutants (<5%) was obtained in presence of the TiO₂ surfaces produced by APS and HVOF sprayings of agglomerated ST01 nanopowder. Other authors reported good photocatalytic responses of APS- or HVOF-sprayed TiO₂ coatings in the decomposition of different organic compounds such as phenol, acetaldehyde, or methylene blue [13–16]. Moreover, the photocatalytic properties of sprayed coatings were improved by the doping of TiO₂ with Pt [30], metallic oxides such as Al₂O₃, Fe₃O₄, ZnO, SnO₂ [31–33], or hydroxyapatite [34]. In our case, the lower-photocatalytic efficiency of APS- and HVOF-sprayed coatings was also correlated with the chemistry and reactivity of nitrogen oxides that are more complex than that of other molecules [35].

When the ST01 powder was injected in aqueous suspension form, the sprayed coating ensured a substantial removal of the nitrogen oxides (around 52% for NO and 34% for NO_x), much higher than that of the powder (31% for NO and 18% for NO_x). High rates of degradation of gaseous pollutants were also recorded in the presence of aqueous suspension plasma sprayed coatings of nonagglomerated nanopowders P25 (around 36% for NO and 15% for NO_x) and PC105 (around 18% for NO and 8% for NO_x), comparable with that measured in the presence of the powders. Meanwhile, a lower degradation of pollutants (8–10%) was obtained for the coating resulting from the plasma spraying of alcoholic suspensions.

The different photocatalytic performances were principally correlated with the crystalline structures of the sprayed coating. Anatase phase was a key parameter in the photocatalytic activity and a higher-anatase ratio with reduced crystallite size allowed a better degradation of nitrogen oxides. Besides, the titania deposits elaborated by the spraying of aqueous ST01 and P25 suspensions provided a higher performance than that of the raw powders. In these cases, the enhanced photocatalytic performance could not be explained considering only the anatase ratio. It was assumed that the removal of the impurities coming from the raw powder elaboration and a cleaning up of the free-water particles when crossing the plasma could explain such behavior. Different techniques of surface investigations (infrared spectroscopy and X-ray photoelectrons spectroscopy) performed on the surface of P25 aqueous suspension sprayed coating [29] showed the presence of a higher hydroxylation compared to that on the raw powder surface. The hydroxyl groups played a beneficial role and enhanced the photocatalytic activity of titania as already reported in the literature [36, 37].

4. CONCLUSION

This paper proposed a comparative study on the microstructure and photocatalytic properties of titanium dioxide coatings obtained by different thermal spray methods: atmospheric plasma spraying, suspension plasma spraying, and high-velocity oxygen fuel process using agglomerated and nonagglomerated TiO₂ nanopowders as feedstock materials. The coatings elaborated by APS and HVOF techniques were characterized by the common lamellar microstructure observed in all thermal sprayed deposits. Besides, the use of ag-

glomerated nanoparticles as feedstock materials involved an important phase transformation from anatase to rutile. The photocatalytic ability for nitrogen oxides was lower than 5% and was correlated principally with the reduced anatase content.

The coatings elaborated by suspension plasma spraying presented a specific structure that depended on the nature of the solvent used in the preparation of the suspensions. The anatase crystalline structure and the crystallite size were preserved in the coatings resulting from an aqueous suspension, whereas a significant phase transformation occurred with alcoholic suspensions. Furthermore, the aqueous suspension sprayed coatings presented a remarkable photocatalytic efficiency that in some conditions was higher than that of the corresponding powder.

It can be concluded that the suspension plasma spraying is an appropriate technique to elaborate active titania surfaces for the photocatalytic reduction of reactive gaseous pollutants such as nitrogen oxides.

ACKNOWLEDGMENT

F.-L. Toma wishes to thank Alexander von Humboldt Foundation (Bonn, Germany) for the research fellowship at Fraunhofer Institute-IWS (Dresden, Germany).

REFERENCES

- [1] A. Fujishima and K. Honda, "Electrochemical photolysis of water at semiconductor electrode," *Nature*, vol. 238, no. 5358, pp. 37–38, 1972.
- [2] D. F. Ollis and H. Al-Ekabi, *Photocatalytic Purification and Treatment of Water and Air, Proceedings of the 1st International Conference*, Elsevier, New York, NY, USA, 1993.
- [3] A. Mills and S. Le Hunte, "An overview of semiconductor photocatalysis," *Journal of Photochemistry and Photobiology A*, vol. 108, no. 1, pp. 1–35, 1997.
- [4] A. Fujishima, T. N. Rao, and D. A. Tryk, "Titanium dioxide photocatalysis," *Journal of Photochemistry and Photobiology C*, vol. 1, no. 1, pp. 1–21, 2000.
- [5] D. C. Hurum, A. G. Agrios, K. A. Gray, T. Rajh, and M. C. Thurnauer, "Explaining the enhanced photocatalytic activity of Degussa P25 mixed-phase TiO₂ using EPR," *Journal of Physical Chemistry B*, vol. 107, no. 19, pp. 4545–4549, 2003.
- [6] T. Ohno, K. Tokieda, S. Higashida, and M. Matsumura, "Synergism between rutile and anatase TiO₂ particles in photocatalytic oxidation of naphthalene," *Applied Catalysis A*, vol. 244, no. 2, pp. 383–391, 2003.
- [7] W. W. Dai, C. X. Ding, J. F. Li, Y. F. Zhang, and P. Y. Zhang, "Wear mechanism of plasma-sprayed TiO₂ coating against stainless steel," *Wear*, vol. 196, no. 1–2, pp. 238–242, 1996.
- [8] R. Gadow and D. Scherer, "Composite coatings with dry lubrication ability on light metal substrates," *Surface and Coatings Technology*, vol. 151–152, pp. 471–477, 2002.
- [9] S. O. Chwa, D. Klein, F.-L. Toma, G. Bertrand, H. Liao, C. Coddet, and A. Ohmori, "Microstructure and mechanical properties of plasma sprayed nanostructured TiO₂-Al composite coatings," *Surface and Coatings Technology*, vol. 194, no. 2–3, pp. 215–224, 2005.
- [10] A. Ibrahim, R. S. Lima, C. C. Berndt, and B. R. Marple, "Fatigue and mechanical properties of nanostructured and conventional titania (TiO₂) thermal spray coatings," *Surface*

- and *Coatings Technology*, vol. 201, no. 16-17, pp. 7589–7596, 2007.
- [11] H. Li, K. A. Khor, and P. Cheang, “Titanium dioxide reinforced hydroxyapatite coatings deposited by high velocity oxy-fuel (HVOF) spray,” *Biomaterials*, vol. 23, no. 1, pp. 85–91, 2002.
- [12] R. S. Lima and B. R. Marple, “Thermal spray coatings engineered from nanostructured ceramic agglomerated powders for structural, thermal barrier and biomedical applications: a review,” *Journal of Thermal Spray Technology*, vol. 16, no. 1, pp. 40–63, 2007.
- [13] C. Lee, H. Choi, C. Lee, and H. Kim, “Photocatalytic properties of nano-structured TiO₂ plasma sprayed coating,” *Surface and Coatings Technology*, vol. 173, no. 2-3, pp. 192–200, 2003.
- [14] A. Ohmori, H. Shoyama, S. Matsusaka, K. Ohashi, K. Moriya, K. Moriya, and C.-J. Li, “Study of photo-catalytic character of plasma sprayed TiO₂ coatings, thermal spray: surface engineering via applied research,” in *Proceedings of the 1st International Thermal Spray Conference*, C. C. Berndt, Ed., pp. 319–323, ASM International, Montréal, Québec, Canada, 2000.
- [15] E.-A. Lee, S.-W. Lee, C.-H. Choi, H.-S. Kim, and B. Hockey, “Effect of TiO₂ powder size on the reactivity of photocatalyst,” *Materials Science Forum*, vol. 439, pp. 288–296, 2003.
- [16] G.-J. Yang, C.-J. Li, F. Han, and A. Ohmori, “Microstructure and photocatalytic performance of high velocity oxy-fuel sprayed TiO₂ coatings,” *Thin Solid Films*, vol. 466, no. 1-2, pp. 81–85, 2004.
- [17] G. Schiller, M. Müller, and F. Gitzhofer, “Suspension plasma spraying for the preparation of perovskite powders and coatings,” in *Thermal Spray: A United Forum for Scientific and Technological Advances*, C. C. Berndt, Ed., pp. 349–352, ASM International, Materials Park, Ohio, USA, 1997.
- [18] P. Blazdell and S. Kuroda, “Plasma spraying of submicron ceramic suspensions using a continuous ink jet printer,” *Surface and Coatings Technology*, vol. 123, no. 2-3, pp. 239–246, 2000.
- [19] K. Wittmann, F. Blein, J. Fazilleau, J.-F. Coudert, and P. Fauchais, “A new process to deposit thin coatings by injecting nanoparticles suspensions in a DC plasma jet,” in *Proceedings of the International Thermal Spray Conference (ITSC '02)*, E. Lugscheider, Ed., pp. 519–522, DVS Düsseldorf, Essen, Germany, March 2002.
- [20] M. Gell, L. Xie, X. Ma, E. H. Jordan, and N. P. Padture, “Highly durable thermal barrier coatings made by the solution precursor plasma spray process,” *Surface and Coatings Technology*, vol. 177-178, pp. 97–102, 2004.
- [21] R. Tomaszek, Z. Znamirowski, L. Pawlowski, and A. Wojnakowski, “Temperature behaviour of titania field emitters realized by suspension plasma spraying,” *Surface and Coatings Technology*, vol. 201, no. 5, pp. 2099–2102, 2006.
- [22] A. Killinger, M. Kuhn, and R. Gadow, “High-velocity suspension flame spraying (HVSFS), a new approach for spraying nanoparticles with hypersonic speed,” *Surface and Coatings Technology*, vol. 201, no. 5, pp. 1922–1929, 2006.
- [23] J. Oberste-Berghaus, J.-G. Legoux, C. Moreau, F. Tarasi, and T. Chráska, “Mechanical and thermal transport properties of suspension thermal sprayed alumina-zirconia composite coatings,” in *Proceedings of the International Thermal Spray Conference and Exposition, Global Coating Solutions (ITSC '07)*, B. R. Marple, M. M. Hyland, Y.-C. Lau, C.-J. Li, R. S. Lima, and G. Montavon, Eds., pp. 627–632, ASM International, Beijing, China, May 2007.
- [24] P. Fauchais, R. Etchart-Salas, C. Delbos, et al., “Suspension and solution plasma spraying of finely structured layers: potential application to SOFCs,” *Journal of Physics D*, vol. 40, no. 8, pp. 2394–2406, 2007.
- [25] J. E. Döring, R. Vaßen, and D. Stöver, “Influence of carrier gas flow and liquid injection in the plasma jet on plasma characteristics during the atmospheric plasma spray process,” in *Proceedings of the International Thermal Spray Conference and Exposition, Advancing the Science & Applying the Technology (ITSC '03)*, C. Moreau and B. Marple, Eds., pp. 641–647, ASM International, Orlando, Fla, USA, May 2003.
- [26] F.-L. Toma, G. Bertrand, S. O. Chwa, C. Meunier, D. Klein, and C. Coddet, “Comparative study on the photocatalytic decomposition of nitrogen oxides using TiO₂ coatings prepared by conventional plasma spraying and suspension plasma spraying,” *Surface and Coatings Technology*, vol. 200, no. 20-21, pp. 5855–5862, 2006.
- [27] N. Berger-Keller, G. Bertrand, C. Filiatre, C. Meunier, and C. Coddet, “Microstructure of plasma-sprayed titania coatings deposited from spray-dried powder,” *Surface and Coatings Technology*, vol. 168, no. 2-3, pp. 281–290, 2003.
- [28] F.-L. Toma, S. Guessasma, D. Klein, G. Montavon, G. Bertrand, and C. Coddet, “Neural computation to predict TiO₂ photocatalytic efficiency for nitrogen oxides removal,” *Journal of Photochemistry and Photobiology A*, vol. 165, no. 1–3, pp. 91–96, 2004.
- [29] F.-L. Toma, G. Bertrand, S. Begin, C. Meunier, O. Barres, D. Klein, and C. Coddet, “Microstructure and environmental functionalities of TiO₂-supported photocatalysts obtained by suspension plasma spraying,” *Applied Catalysis B*, vol. 68, no. 1-2, pp. 74–84, 2006.
- [30] Y. Zeng, W. Wu, S. Lee, and J. Gao, “Photocatalytic performance of plasma sprayed Pt-modified TiO₂ coatings under visible light irradiation,” *Catalysis Communications*, vol. 8, no. 6, pp. 906–912, 2007.
- [31] A. Ohmori, F.-X. Ye, and C.-J. Li, “The effects of the additives on photocatalytic performance of plasma sprayed titanium dioxide coatings,” in *Proceedings of the International Thermal Spray Conference, (ITSC '02)*, E. Lugscheider, Ed., pp. 165–169, DVS Düsseldorf, Essen, Germany, March 2002.
- [32] Y. Zeng, J. Liu, W. Wu, and C. Ding, “Photocatalytic performance of plasma sprayed TiO₂-ZnFe₂O₄ coatings,” *Surface and Coatings Technology*, vol. 200, no. 7, pp. 2398–2402, 2005.
- [33] H. Chen, S. W. Lee, T. H. Kim, and B. Y. Hur, “Photocatalytic decomposition of benzene with plasma sprayed TiO₂-based coatings on foamed aluminum,” *Journal of the European Ceramic Society*, vol. 26, no. 12, pp. 2231–2239, 2006.
- [34] F.-X. Ye, A. Ohmori, T. Tsumura, K. Nakata, and C.-J. Li, “Microstructures and compositions of photocatalytic plasma-sprayed titania-hydroxyapatite coatings,” in *Proceedings of the International Thermal Spray Conference and Exposition, Global Coating Solutions (ITSC '07)*, B. R. Marple, M. M. Hyland, Y.-C. Lau, C.-J. Li, R. S. Lima, and G. Montavon, Eds., pp. 341–346, ASM International, Beijing, China, May 2007.
- [35] G. Brasseur, *Physique et chimie de l'atmosphère moyenne*, Masson, Paris, France, 1982.
- [36] J. S. Dalton, P. A. Janes, N. G. Jones, J. A. Nicholson, K. R. Hallam, and G. C. Allen, “Photocatalytic oxidation of NO_x gases using TiO₂: a surface spectroscopic approach,” *Environmental Pollution*, vol. 120, no. 2, pp. 415–422, 2002.
- [37] S. Devahasdin, C. Fan Jr., K. Li, and D. H. Chen, “TiO₂ photocatalytic oxidation of nitric oxide: transient behavior and reaction kinetics,” *Journal of Photochemistry and Photobiology A*, vol. 156, no. 1-3, pp. 161–170, 2003.



Hindawi

Submit your manuscripts at
<http://www.hindawi.com>

